

## Surface Studies of Solids by Total Reflection of X-Rays\*

L. G. PARRATT

Cornell University, Ithaca, New York

(Received March 22, 1954)

Analysis of the shape of the curve of reflected x-ray intensity *vs* glancing angle in the region of total reflection provides a new method of studying certain structural properties of the mirror surface about 10 to several hundred angstroms deep. Dispersion theory, extended to treat any (small) number of stratified homogeneous media, is used as a basis of interpretation.

Curves for evaporated copper on glass at room temperature are studied as an example. These curves may be explained by assuming that the copper (exposed to atmospheric air at room temperature) has completely oxidized about 150Å deep. If oxidation is less deep, there probably exists some general reduction of density (e.g., porosity) and an electron density minimum just below an internal oxide seal. This seal, about 25Å below the nominal surface plane, arrests further oxidation of more deeply-lying loose-packed copper crystallites.

All measurements to date have been carried out under laboratory atmospheric conditions which do not allow satisfactory separation or control of the physical and chemical variables involved in the surface peculiarities. The method, under more controlled conditions of preparation and treatment of the surface, promises to be useful.

## I. INTRODUCTION

SINCE x-rays in total reflection from a mirror surface penetrate very little into the mirror medium, peculiarities in the reflected intensity reveal structural peculiarities of the surface itself. Analysis of the reflected intensity may provide a new and fruitful method for studying surface properties that involve variations of electron density with depth, e.g., corrosion, porosity, aging, or annealing, and perhaps for studying smoothness on a scale between that of the optical microscope and the electron microscope.

A typical experimental arrangement for this method is sketched in Fig. 1. The intensity reflected from a smooth surface of a thick mirror of glass, for example, varies with the incident glancing angle  $\phi$  as shown in Fig. 2 for an x-ray wavelength 1.39Å (the Cu  $K\beta_1$  line). For this curve, the observed cut-off or critical angle  $\phi_c$  is 12.3 minutes of arc or  $3.58 \times 10^{-3}$  radian.

The critical angle and the shape of the observed curve are determined essentially by the electron density and are otherwise independent of the amorphous or crystalline structure, or of the orientation of crystallites on (or in) the surface. If the mirror interface is a sharply defined boundary between two uniform homogeneous media, the dispersion theory predicts the reflection curve. The predicted curve for air and glass is shown

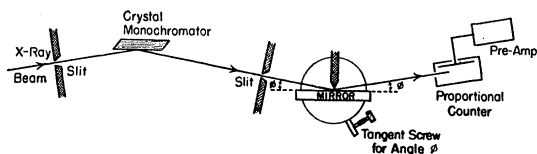


FIG. 1. Experimental arrangement for the x-ray total reflection method of studying smooth solid surfaces.

\* This research was supported by the United States Air Force through the Office of Scientific Research of the Air Research and Development Command.

in Fig. 2. In general, the experimental and theoretical curves are in qualitative but not detailed agreement.

The proposed method consists of (1) a comparison of an observed curve with a theoretical curve, and/or (2) a comparison of the observed curves for differently produced surfaces, or for a given surface before and after some specific treatment. The shape of the theoretical curve depends sensitively upon the particular model one chooses for the surface; by adjusting the model to give a theoretical curve in closer agreement with experiment, one learns which properties of the surface are responsible for the various peculiarities of the observed curve.

In the present paper, the theory is outlined and a few exemplary experimental curves are discussed, in particular a curve for evaporated copper on a glass substrate. Some quantitative results and conclusions are possible but satisfactory utilization of this method must await (as must most other methods for the study of surfaces) improved experimental techniques in the production and control of the surfaces.

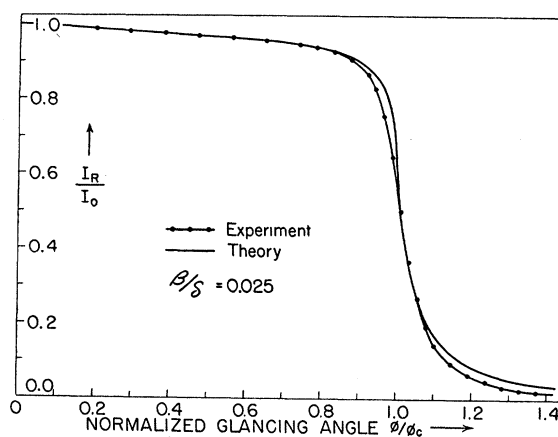


FIG. 2. Intensity reflected from polished glass at small angles of incidence. The angle  $\phi_c$  is the critical angle for total reflection.

II. DISPERSION THEORY

Two Homogeneous Media

For any glancing angle, the expressions for the electric vector of the incident beam  $E_1(z_1)$ , of the reflected beam  $E_1^R(z_1)$ , and of the refracted beam  $E_2(z_2)$  at a perpendicular distance  $z$  from the surface, are

$$\left. \begin{aligned} E_1(z_1) &= E_1(0) \exp\{i[\omega t - (k_{1,x}x_1 + k_{1,z}z_1)]\} \\ E_1^R(z_1) &= E_1^R(0) \exp\{i[\omega t - (k_{1,x}x_1 - k_{1,z}z_1)]\} \\ E_2(z_2) &= E_2(0) \exp\{i[\omega t - (k_{2,x}x_2 + k_{2,z}z_2)]\} \end{aligned} \right\}, \quad (1)$$

where  $k_1$  and  $k_2$  are the propagation vectors (of magnitudes  $2\pi/\lambda_1$  and  $2\pi/\lambda_2$ ) outside and inside the mirror, respectively,  $z$  is taken as positive into the mirror,  $x, z$  is the plane of incidence, refraction, and reflection of the beam, and the athwart direction  $y$  is parallel to the mirror surface. For x-rays, the glancing angle  $\phi_1$  (written hereafter without the subscript) is always very small, and we write

$$k_{2,x}^2 + k_{2,z}^2 = k_2^2 = r_2^2 k_1^2 = r_2^2 (k_{1,x}^2 / \cos^2 \phi) \doteq k_{1,x}^2 (1 - 2\delta_2 - 2i\beta_2 + \phi^2),$$

where  $r_2 = 1 - \delta_2 - i\beta_2$  is the refractive index of the mirror,  $r_1 = 1$  for air or vacuum, and where we neglect second and higher powers of  $\delta_2$  and  $\beta_2$  since they are each of the order of  $10^{-5}$  or less.  $\beta_2 = \lambda\mu_2/4\pi$  where  $\mu_2$  is the linear (incoherent) absorption coefficient of the mirror.

From the boundary condition for the tangential components of the electric vectors,  $k_{2,x} = k_1$ , and with the approximation  $k_{1,x} \doteq k_1$  for small  $\phi$ , it follows that

$$k_{2,z} \doteq k_1 (\phi^2 - 2\delta_2 - 2i\beta_2)^{\frac{1}{2}}.$$

For convenience, we write

$$f_2 = (\phi^2 - 2\delta_2 - 2i\beta_2)^{\frac{1}{2}}.$$

The expression for the refracted beam becomes

$$E_2(z_2) = E_2(0) \exp[i(\omega t - k_{2,x}x_2)] \exp[-ik_{1z}f_2z_2]. \quad (2)$$

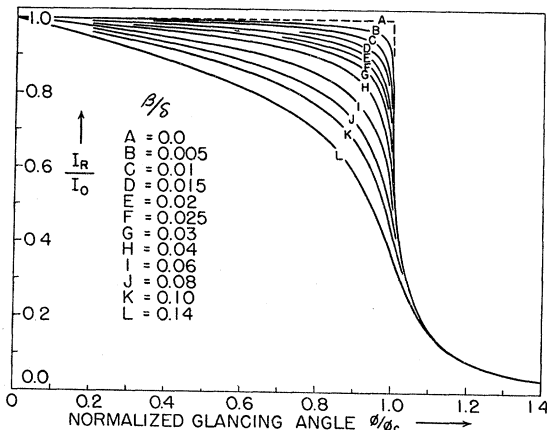


FIG. 3. Two-media theoretical reflection curves for selected values of  $\beta/\delta$ . The shape depends upon the absorption of x-rays in the mirror. For no absorption, the reflection coefficient is unity for  $0 < \phi/\phi_c < 1$ , then drops abruptly.

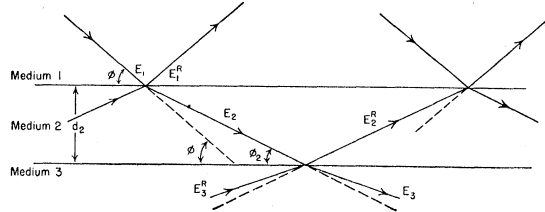


FIG. 4. Sketch of reflection and refraction for stratified homogeneous media.

Shape of the Reflection Curve: Two Media

The Fresnel<sup>1</sup> coefficient for reflection,  $F_{1,2}$ , can be written

$$F_{1,2} = \frac{E_1^R}{E_1} = \frac{\sin\phi - r_2 \sin\phi_2}{\sin\phi + r_2 \sin\phi_2} \doteq \frac{\phi - f_2}{\phi + f_2} = \frac{f_1 - f_2}{f_1 + f_2}, \quad (3)$$

where

$$f_1 = (\phi^2 - 2\delta_1 - 2i\beta_1)^{\frac{1}{2}} = \phi.$$

The first part of Eq. (3) is written for the  $\sigma$  component of polarization, but, within the approximations made in the second part, no distinction need be made between the  $\sigma$  and  $\pi$  components.

To obtain the expression for the intensity ratio, we write

$$f_2 = A - iB,$$

where

$$A = \frac{1}{\sqrt{2}} \{ [(\phi^2 - \phi_{c2}^2)^2 + 4\beta_2^2]^{\frac{1}{2}} + (\phi^2 - \phi_{c2}^2)^{\frac{1}{2}} \},$$

$$B = \frac{1}{\sqrt{2}} \{ [(\phi^2 - \phi_{c2}^2)^2 + 4\beta_2^2]^{\frac{1}{2}} - (\phi^2 - \phi_{c2}^2)^{\frac{1}{2}} \},$$

and from Snell's law, *viz.*,  $r_2 = \cos\phi/\cos\phi_2$ , we write  $\delta_2 = \frac{1}{2}\phi_{c2}^2$  where  $\phi_{c2}$  is the critical angle of incidence for which the angle inside the mirror is just zero. Inserting these relations in Eq. (3) and multiplying the numerator and denominator by the complex conjugate, we get the ratio of reflected to incident intensity,

$$\frac{I_R}{I_0} = \left| \frac{E_1^R}{E_1} \right|^2 = \frac{(\phi - A)^2 + B^2}{(\phi + A)^2 + B^2} = \frac{h - (\phi/\phi_{c2})\sqrt{2}(h-1)^{\frac{1}{2}}}{h + (\phi/\phi_{c2})\sqrt{2}(h-1)^{\frac{1}{2}}}, \quad (4)$$

where

$$h = \left( \frac{\phi}{\phi_{c2}} \right)^2 + \left\{ \left[ \left( \frac{\phi}{\phi_{c2}} \right)^2 - 1 \right]^2 + \left( \frac{\beta}{\delta} \right)^2 \right\}^{\frac{1}{2}}.$$

Equation (4) is plotted for each of several values of  $\beta/\delta$  in Fig. 3. The value 0.025 gives the "best match" with the observed curve for the glass mirror, and is the value used in the theoretical curve of Fig. 2.

<sup>1</sup> E.g., A. H. Compton and S. K. Allison, *X-Rays in Theory and Experiment* (D. Van Nostrand Company, Inc., New York, 1935), p. 307. Fresnel theory for homogeneous media is presumed to hold for "granular" matter even though the x-ray wavelengths are of the order of magnitude of the atomic "grain" size: The penetration of the x-rays (discussed later) is large compared with this "grain" size.

### *N* Stratified Homogeneous Media

One conjecture as to the difference between the experimental and the two-media theoretical curves for a metal surface involves the role of a possible oxide surface layer. Another conjecture, in case the surface material is deposited as a thin film on a substrate of different material, involves the effect of the substrate. Other conjectures may involve a complicated model of the surface structure that requires more than two laminal media for representation. So, we next derive the theoretical expression for the shape of the reflection curve for *N* ( $N \geq 2$ ) stratified homogeneous media having smooth boundary interfaces.

We denote the thickness of each lamina *n* ( $n \leq N$ ) by  $d_n$ . The thickness of medium 1 (air or vacuum) is of no concern.

The continuity of the tangential components of the electric vectors (see Fig. 4) for the  $n-1, n$  boundary may be expressed as

$$a_{n-1}E_{n-1} + a_{n-1}^{-1}E_{n-1}^R = a_n^{-1}E_n + a_n E_n^R, \quad (5)$$

$$(a_{n-1}E_{n-1} - a_{n-1}^{-1}E_{n-1}^R)f_{n-1}k_1 = (a_n^{-1}E_n - a_n E_n^R)f_n k_1, \quad (6)$$

where the amplitude factor  $a_n$  for half the perpendicular depth  $d_n$  is, from Eq. (2),

$$a_n = \exp\left(-ik_1 f_n \frac{d_n}{2}\right) = \exp\left(-i \frac{\pi}{\lambda} f_n d_n\right). \quad (7)$$

In Eqs. (5) and (6), the vector amplitudes  $E_{n-1}$ ,  $E_{n-1}^R$  and  $E_n$ ,  $E_n^R$  refer to the values midway through medium  $n-1$  and  $n$ , respectively.

The solution of the simultaneous Eqs. (5) and (6) is obtained by dividing their difference by their sum and

TABLE I. Penetration  $z_{1/e}$  in copper, in A. [ $I_2(z_{1/e})/I_2(0) = 1/e$ ]

$\phi/\phi_c$	1.281A	1.392A	1.540A
0.10	17.7	18.6	17.8
0.25	18.2	19.1	18.3
0.50	20.3	21.4	20.4
0.75	26.3	28.0	26.7
0.90	38.2	42.4	40.5
0.95	48.1	59.0	56.2
0.99	62.0	118	111
1.00	66.5	181	164
1.01	71.4	276	243
1.05	93.3	567	490
1.10	121	808	699
1.20	168	1170	1008
1.30	209	1464	1263
1.40	246	1724	1489
$\delta =$	$16.72 \times 10^{-6}$	$17.85 \times 10^{-6}$	$24.05 \times 10^{-6}$
$\beta =$	$23.5 \times 10^{-7}$	$3.76 \times 10^{-7}$	$5.58 \times 10^{-7}$

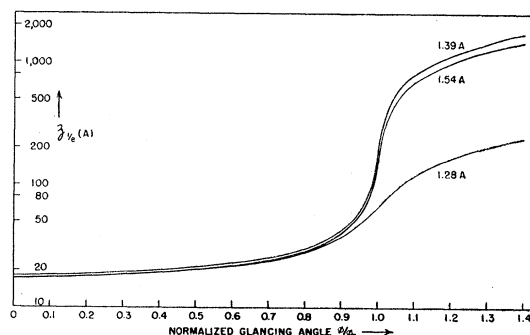


FIG. 5. Calculated  $1/e$  penetration depths in copper. Penetration is very small for  $\phi/\phi_c \lesssim 0.9$  and here is not sensitive to the photoelectric absorption coefficient. For  $\phi/\phi_c > 1$  the penetration is given essentially by the usual absorption relation.

writing the result as a recursion formula

$$R_{n-1, n} = a_{n-1}^4 \left[ \frac{R_{n, n+1} + F_{n-1, n}}{R_{n, n+1} F_{n-1, n} + 1} \right], \quad (8)$$

where

$$R_{n, n+1} = a_n^2 (E_n^R / E_n)$$

and

$$F_{n-1, n} = \frac{f_{n-1} - f_n}{f_{n-1} + f_n}.$$

One solves Eq. (8) for  $E_1^R/E_1$  by starting at the bottom medium, medium *N*, and noting that  $R_{n, n+1} = 0$  since the thickness of this medium is infinite. One also notes that  $a_1$  is unity, and therefore  $R_{1, 2} = E_1^R/E_1$ .

The ratio of reflected to incident intensity,  $I_R/I_0$ , is obtained by separating Eq. (8) for  $R_{1, 2}$  into its real and imaginary terms and multiplying by the complex conjugate. This step is symbolized by

$$I_R/I_0 = |E_1^R/E_1|^2. \quad (9)$$

The algebra is straightforward but very tedious for  $N > 3$ . Evaluations of Eq. (9) for *N* up to 6 have been carried out and are discussed later.

### Penetration: Two Media

So that we may have some quantitative idea of the thickness of the surface layer involved, we shall determine the theoretical depth of penetration of the x-ray beam in medium 2 when  $d_2 = \infty$ .

The expression for the refracted beam is given by Eq. (2). For the intensity at depth *z*, we multiply the exponent by its complex conjugate. The depth  $z_{1/e}$  at which the intensity is reduced to  $1/e$  is readily seen to be

$$z_{1/e} = \lambda/4\pi B. \quad (10)$$

Calculations with Eq. (10) for three wavelengths for a copper mirror are listed in Table I and are plotted in Fig. 5. The  $\delta$  and  $\beta$  values indicated in the table are the normal bulk copper values, taken from Table II. Note that wavelengths are selected on either side of the *K*-absorption discontinuity  $\lambda_K = 1.379\text{A}$ , so that

TABLE II. Calculations for  $\delta$  for copper.

Line	$\lambda(\text{A})$	$\lambda/\lambda_K$	$g_K \text{Re}(J_K-1)$	$g_{L_I} \text{Re}(J_{L_I}-1)$	$g_{L_{II,III}} \text{Re}(J_{L_{II,III}}-1)$	$g_M \text{Re}(J_M-1)$	$\delta(\times 10^6)$
WL $\beta_1$	1.281	0.930	-2.340	-0.017	0.170	0.030	16.72
CuK $\beta_1$	1.392	1.010	-4.949	-0.020	0.190	0.034	17.85
CuK $\alpha_1$	1.541	1.117	-2.565	-0.025	0.213	0.039	24.05
	$\lambda_K = 1.379\text{A},$ $\lambda_{L_I} = 12.0,$ $\lambda_{L_{II,III}} = 13.15,$ $\lambda_M = 160,$		$p_K = 11/4,$ $p_{L_I} = 2.0,$ $p_{L_{II,III}} = 5/2,$ $p_M = 5/2,$	$g_K = 1.33,$ $g_{L_I} = 1.5,$ $g_{L_{II,III}} = 4.0,$ $g_M = 20.$		$\rho = 8.936 \text{ g/cm}^3,$ $M = 63.57 \text{ g/mole},$	

the linear absorption coefficients are different by a factor of more than 6. Until  $\phi/\phi_c$  becomes very close to unity, the thickness of the layer involved in the reflection process is small, of the order of 20 to 50A. After the critical angle is reached, the penetration depth becomes rapidly large and is soon the value calculated from the familiar absorption relation,

$$\frac{I_2(z_{1/e})}{I_2(0)} \doteq \exp(-\mu_2 z_{1/e}) \doteq \exp\left[-\frac{\mu_2}{\phi_2} z_{1/e}\right]$$

$$= \exp\left[-\frac{\mu_2}{(\phi^2 - 2\delta_2)^{1/2}} z_{1/e}\right].$$

Actually, the *effective* thickness for our interest in reflected intensity is even less than  $z_{1/e}$  (especially since the involvement is weighted exponentially with depth), the top surface layer being much more important than successively deeper layers.

However, as discussed later, the mirror is probably not homogeneous. For example, porosity, or an oxide layer on copper, would cause the penetration [for  $I_2/I_2(0) = 1/e$ ] to be somewhat greater than the calculated value.

### Theoretical Values of $\delta$

The quantum-mechanical theory for the complex refractive index, in terms of the various  $q$  shells of electrons, gives

$$r = 1 - \delta - i\beta = 1 - A'\lambda^2 \frac{\rho}{M} \sum_q \int_{\omega_q}^{\infty} \frac{\omega^2 (dg/d\omega)_q}{\omega^2 - \omega_q^2 - i\eta_q \omega} d\omega, \quad (11)$$

where

$$A' = Ne^2/2\pi m_e c^2 \doteq 2.7019 \times 10^{10},$$

$N$  = Avogadro's number;  $e$  = electronic charge;  $m_e$  = electronic mass;  $c$  = velocity of light;  $\rho$  = density;  $M$  = molecular weight;  $\omega = 2\pi\nu$ ,  $\nu$  = incident x-ray frequency;  $\omega_q = 2\pi\nu_q$ ,  $\nu_q$  = frequency of dispersion oscillators;  $\omega_q = 2\pi\nu_q$ ,  $\nu_q$  = frequency of the  $q$ -absorption discontinuity;  $(dg/d\omega)_q$  = density of dispersion oscillators,  $q$ -type electrons, near  $\omega_q$ ; and  $\eta_q$  = damping factor. The density of the dispersion oscillators follows the absorption relation  $\lambda^{p_q}$  for  $q$ -type electrons, and the area under the curve of the absorption spectrum gives the oscillator strength  $g_q$ . The damping factor  $\eta_q$  is given by a combination of the classical radiation damping and the

width of the  $q$  state: For copper and the wavelengths of the present work, the damping factor is safely neglected.<sup>2</sup>

The real part of the integral term of Eq. (11) gives

$$\delta = A'\lambda^2 \frac{\rho}{M} [Z + g_K \text{Re}(J_K-1) + g_{L_I} \text{Re}(J_{L_I}-1) + g_{L_{II,III}} \text{Re}(J_{L_{II,III}}-1) + g_M \text{Re}(J_M-1)], \quad (12)$$

where  $A'\lambda^2(\rho Z/M)$  is the normal dispersion term ( $Z$  is the atomic number), and the others are the significant anomalous dispersion terms for copper at  $\lambda = 1.39\text{A}$ . The real part of  $(J_q-1)$  is shown integrated in reference 2.

Calculations for  $\delta$  are listed in Table II. The various constants used in these calculations are given under the table and are discussed in reference 2.

### III. EXPERIMENTAL CURVES

A moderately thick (about 2000A) copper film was deposited by evaporation<sup>3</sup> on the glass surface studied in Fig. 2. OFHC copper (pieces of 25-mil wire) was evaporated during a time of about 20 minutes from an array of four 15-mil tantalum helical filaments 20 cm from the substrate and spaced linearly to give a film of very nearly uniform thickness along the 14-cm surface. The curve recorded for this film with the Cu K $\beta_1$  line,  $\lambda = 1.39\text{A}$ , is shown in Fig. 6.

The experimental curve of Fig. 6 is typical of about 30 copper curves, with many different moderately thick films and different glass substrates, that have been

<sup>2</sup> L. G. Parratt and C. F. Hempstead, Phys. Rev. **94**, 1593 (1954).

<sup>3</sup> The optically polished glass surface was cleaned as follows: Washed thoroughly with Lakesal laboratory soap, rinsed with tap water, swabbed with 30 percent hydrogen peroxide (CP), stroked lightly with a cheesecloth swab soaked with acetone (CP) several times until no "breath figure" could be seen, then, finally, subjected in the vacuum to a glow discharge for several minutes.

No special effort was made in the present work to control the rate of evaporation or condensation, temperature of the substrate during or after the condensation, traces of gases and of unidentified material on the substrate or in the evaporation chamber, nor subsequent adsorption or chemisorption on the surface.

Backstreaming of the pumping fluid, Octoil S, was reduced by two water-cooled baffles in series in the pumping line. A liquid N<sub>2</sub> trap was supported inside the evacuation chamber.

The pressure during evaporation was always less than  $10^{-6}$  mm Hg, and about  $3 \times 10^{-7}$  before and after evaporation, as measured with a Bayard-Alpert type ionization gauge.

recorded with  $\lambda=1.39\text{\AA}$ , and of about 20 curves with  $\lambda=1.54\text{\AA}$ . (Films of mean thickness less than about 200\text{\AA} show special features which will be discussed in a later paper.) The Fig. 6 curve is also more or less typical of many gold, silver, and aluminum mirrors.

In this Section we consider four general problems in the interpretation of an experimental curve: (1) instrumental effects, (2) smoothness of the mirror, (3) matching the two-media theoretical curve to the experimental curve, and (4) the experimental value of  $\delta$ .

### Instrumental Effects

The observed curve, especially in the region of maximum slope, is of course perturbed to some extent by such instrumental effects as imperfect collimation and heterochromaticity of the incident x-ray beam, and any inaccuracy in either coordinate scale. These effects are believed to be negligibly small in the present work.

The beam was collimated and monochromatized by (1) a slit 0.01 cm wide placed near the x-ray tube and 37 cm from the calcite monochromator crystal, see Fig. 1, (2) the diffraction pattern of the calcite crystal (about 11 seconds full width at half-maximum), and (3) a second slit 0.003 cm wide placed between the crystal and the mirror at a position 23 cm from the axis of the crystal. The second slit, about 1 cm from the near end of the mirror, served to cut off the angular and spectroscopic "tails" of the beam and also to reduce the linear width of the beam incident on the mirror. The mirror subtended the entire beam at  $\phi \geq 1 \times 10^{-3}$  radian.

Although the x-ray tube was operated at 35 kv, the spectral pass band, less than one x.u. wide at half-maximum, was so narrow that we can safely ignore the continuous radiation in higher orders of Bragg reflection from the calcite crystal.

The incident angle  $\phi$  was measured on the drum of a tangent micrometer screw. Increments in  $\phi$  were accurate to better than 2 seconds of arc. The zero of the angle scale was determined from photographs of the direct beam and of the reflected beam with each of several values of  $\phi$  as follows: Measurements of the distances between the photographic images were made with a comparator and the zero angle obtained by extrapolation. The zero angle accuracy was about  $\pm 4$  seconds of arc.

The intensity scale (response of the proportional counter system<sup>4</sup>) was found to be linear within 0.5 percent if the counting rate did not exceed 1000 counts per second (5-microsecond resolving time).

<sup>4</sup>We have also used Geiger counter and ionization chamber systems. A proportional counter system with a resolving time less than 5 microseconds is recommended. Geiger counter systems were found unsatisfactory [Parratt, Hempstead, and Jossem, *Rev. Sci. Instr.* **23**, 1 (1952)], and the ionization chamber method has an unfavorable combination of sensitivity, stability and response time. The proportional system, with a channel discriminator as we use it, provides a very effective method for reducing the magnitude of the background intensity.

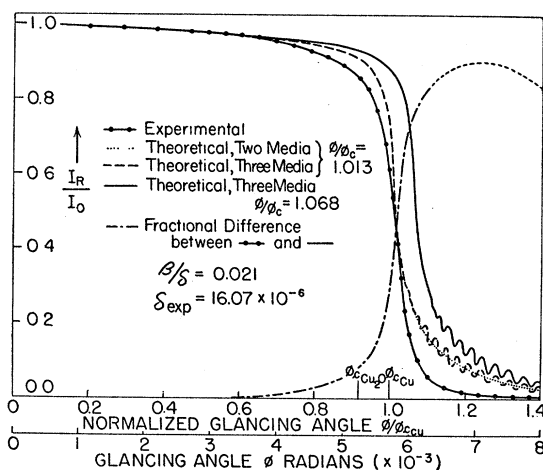


Fig. 6. Comparison of experimental and theoretical reflection curves for copper (2000\text{\AA} thick) on glass for  $\lambda=1.39\text{\AA}$ . The experimental surface is evaporated copper on polished glass. In the normalized abscissas scale,  $\phi_c$  is the experimental value. Explanation of the difference between the curves involves conjectures as to peculiarities of the experimental surface.

(The maxima and minima for  $\phi/\phi_c > 1$ , three media curve, comprise an interference pattern between beams reflected from the copper and from the glass substrate.)

The incident intensity was measured by recording the direct beam with the mirror temporarily slid out of position.

### Mirror Smoothness

Lack of smoothness of the mirror is probably most sensitively detected in the region of maximum slope of the curve. The theoretical curves are based on a surface model of perfect smoothness, so a comparison of the experimental and theoretical curves, properly matched for  $\beta/\delta$ , should provide a first test for smoothness.

Since the curves of Fig. 2 show very satisfactory agreement at the inflection point, the glass substrate appears to be smooth.<sup>5,6</sup> The maximum slopes of the experimental and theoretical curves for copper, Fig. 6, are also in rather satisfactory agreement but the experimental slope is slightly smaller than the theoretical.

<sup>5</sup>The curve of Fig. 2 was taken with a glass mirror optically flat to about a tenth of a wavelength of green light over the critical central few centimeters, and to one wavelength over the full length, 14 cm, of the mirror. Flatness to about 500\text{\AA} is necessary to avoid reflection distortion [see C. M. Lucht and D. Harker, *Rev. Sci. Instr.* **22**, 392 (1951)].

<sup>6</sup>Electron microscope studies show freshly polished glass surfaces with a smoothness of about 10\text{\AA} over very short distances, and infrequent scratch grooves as deep as 500\text{\AA} [R. C. Williams and R. C. Backus, *J. Appl. Phys.* **20**, 98 (1949)]. Multiple-beam interferometry shows surface planeness to within 1/150 of a wavelength (of visible radiation) over a test area of about 4-mm diameter [O. S. Heavens, *Proc. Phys. Soc. (London)* **B64**, 419 (1951)].

However, over a few thousand angstroms extent along at least some optically polished glass mirrors, x-ray reflection work by W. Ehrenberg, *J. Opt. Soc. Am.* **39**, 746 (1949), has indicated a ripple-type of surface with peak to trough depth about 10\text{\AA} and a ripple length of about 2 mm. Such ripple structure, if present, would give some broadening of the inflection part of the observed curve.

Possibly the copper surface is not quite as smooth as the glass but, alternatively, the difference in slope could be caused by a nonuniform electron density of the mirror medium as discussed later.

As another check on smoothness of the copper mirror, microdensitometer analyses of photographs of both the direct and reflected beams were made. An appreciable change in shape or an increase in width of the beam upon reflection would indicate mirror roughness. No significant difference in shape or width was detected, a conclusion in agreement with Kiessig<sup>7</sup> on nickel films.

It is at first surprising that any experimental surface appears smooth to x-rays. One frequently hears that, for good reflection, a mirror surface must be smooth to within about one wavelength of the radiation involved.<sup>8</sup> This condition, applicable for visible radiation at large glancing angles, apparently does not apply for x-rays at very small glancing angles.

### Best Match of Curves

With spurious instrumental factors and mirror roughness discounted, the shape of the observed curve must be explained in terms of some model of the mirror structure. Without prior knowledge of the actual structure, we shall assume the simplest model, *viz.*, two homogeneous media with a sharp plane interface. The difference between the experimental curve and a *matched* two-media curve, with conjectures as to a better model, is discussed later. First, we must effect the two-media match, i.e., for a homogeneous copper lamina on a glass substrate.

In the region  $\phi/\phi_c \lesssim 0.6$ , the experimental and theoretical curves, Fig. 6, are both rather flat. In this region, we have essentially total reflection from any electron density greater than about 40 percent of the normal bulk copper value. This is a reasonable density limit with any surface model later considered, so we expect that here the curves should match. We match also at one point<sup>9</sup> in the inflection region, at, say,  $I_R/I_0 = \frac{1}{2}$  (which point we shall call  $\phi_{\frac{1}{2}}$ ), but we do not try to match the maximum slope. With these match criteria, we find that the ratio  $\beta/\delta$  is rather rigidly fixed.

If the actual electron density in the mirror is not constant with depth, the intensity match at  $\phi_{\frac{1}{2}}$  (i.e., at  $\phi/\phi_c = 1.013$  as shown later) is not quite consistent with the  $\phi/\phi_c \lesssim 0.6$  match. For example, if the density increases with depth, the effective penetration of the x-ray beam would cause the curve in the region  $\phi/\phi_c \lesssim 1$  to be somewhat lower than the theoretical two-media curve matched at  $\phi/\phi_c = 1.013$ . (Of course, in the

match,  $\phi_c$  is the experimental value; if the value for the normal bulk copper were used, the theoretical curve would pass through  $\phi_{\frac{1}{2}}/\phi_c = 1.068$ ; this curve for three media is also shown in Fig. 6.) However, a few percent uncertainty as to the proper  $\phi/\phi_c$  value at which to make the match in the inflection region is of little moment so far as the  $\beta/\delta$  value is concerned.

It is interesting to check the matching value of  $\beta/\delta$  with the ratio obtained from the normal bulk values.<sup>10</sup> These values, from Table I, give  $\beta/\delta = 0.021$ , in perfect agreement with the matching value.

A three-media curve, Eq. (8), for 2000Å normal bulk copper on glass differs from the two-media curve by including the effect of penetration to, and reflection from, the glass. The three-media curve does not differ significantly from the two-media curve in the match regions, but in the region  $\phi/\phi_c > 1$  the curve oscillates in an interference pattern.<sup>11</sup> In Fig. 6, both the matched two- and three-media curves are shown.

### Experimental $\delta$

Use of the normalized abscissa scale  $\phi/\phi_c$  in Figs. 2 and 6 implies prior knowledge of the value of  $\phi_c$  (or of  $\delta$ ). With the value of  $\beta/\delta$  from the "best match" just discussed, a rather precise value of  $\phi_c$  may be read from the  $\phi$  curve by the following method. With the experimental point  $\phi_{\frac{1}{2}}$ , easily and unambiguously determined, and with the value of  $\beta/\delta$ , we obtain  $\phi_c$  from Eq. (13) which is a version of Eq. (4).

$$\frac{\phi_{\frac{1}{2}}}{\phi_c} = \left\{ \frac{1 + (\beta/\delta)^2}{1 + 9(\beta/\delta)^2} \left[ \frac{1}{2} + \frac{3\sqrt{2}}{8} (1 + (\beta/\delta)^2)^{\frac{1}{2}} \right] \right\}^{\frac{1}{2}}. \quad (13)$$

The ratio  $\phi_{\frac{1}{2}}/\phi_c$  is not a sensitive function of  $\beta/\delta$ , as can be seen from Table III, and the uncertainty in the "best match" estimate of  $\beta/\delta$  is usually not serious. In case this uncertainty is significant, we may make a new plot with  $\phi/\phi_c$  as abscissas, using the tentative value of  $\phi_c$ , and effect a better "best match," i.e., a more accurate value of  $\beta/\delta$  and, from Eq. (13), a final value of  $\phi_c$ .

An experimental precision better than 1 percent is practical in the determination of  $\delta$  ( $= \frac{1}{2}\phi_c^2$ ).

From the experimental curve of Fig. 6,  $\beta/\delta = 0.021$  and  $\phi_{\frac{1}{2}} = (19.78 \pm 0.1)$  minutes of arc; we calculate from Eq. (13) that  $\phi_{\frac{1}{2}}/\phi_c = 1.013$  and deduce  $\phi_c = 19.5$  minutes or  $5.67 \times 10^{-3}$  radian. From this  $\phi_c$ ,  $\delta = (16.07 \pm 0.2) \times 10^{-6}$  for copper for  $\lambda = 1.39\text{Å}$ .

Of course, if the electron density in the mirror is not

<sup>7</sup> H. Kiessig, Ann. Physik 10, 715 (1931).

<sup>8</sup> Electron diffraction studies of evaporated copper surfaces show randomly oriented single crystallites of about 70Å or more on an edge [e.g., see H. Levinstein, J. Appl. Phys. 20, 306 (1949), and references].

<sup>9</sup> It is common practice to assume this match point in determining  $\delta$ . E.g., see reference 7; A. J. Lameris and J. A. Prins, Physica 1, 881 (1934), and references.

<sup>10</sup> Normal bulk values may be used in this check since (a) both  $\beta$  and  $\delta$  vary linearly with density, and (b) the shape of the theoretical curve depends only upon the ratio  $\beta/\delta$  [see Eq. (4)].

<sup>11</sup> No significant oscillations were observed in the experimental curve of Fig. 6, although, when recorded with more closely-spaced points, some curves do show faint oscillations.

The oscillating interference pattern is more pronounced with films somewhat thinner than 2000Å. See also H. Kiessig, Ann. Physik 10, 769 (1931); F. Odenbach, Ann. Physik 38, 469 (1940); and R. Riedmiller, Ann. Physik 20, 377 (1934).

TABLE III. Calculations from Eq. (13).

$\beta/\delta$	0	0.02	0.03	0.04	0.06	0.08	0.10	0.12	0.14	0.18
$\phi_i/\phi_c$	1.015	1.013	1.011	1.009	1.007	0.991	0.976	0.961	0.947	0.911

constant with depth, the experimental  $\delta$  corresponds to some sort of average density over the depth penetrated by the x-ray beam.

#### IV. CONJECTURES ABOUT SURFACE PROPERTIES

The experimental value of  $\delta$  for the copper surface is 10 percent less than the normal bulk copper value. Therefore, with no intent now to match the experimental curve in the inflection region, we should draw the three-media curve for 2000Å copper on glass through the point  $\phi/\phi_c=1.068$  where  $\phi_c$  is the experimental value. This is the solid curve in Fig. 6. The discrepancy between the experimental curve and this solid curve is shown as the fractional difference, the short-long dash curve. In this section we shall conjecture as to the properties of the surface responsible for this difference.

Before proceeding to specific structural models of the surface, let us inquire as to a likely *a priori* general nature of the surface.

#### Spongy Surface Structure

During the production of a copper mirror by evaporation and condensation onto a polished glass substrate, we suppose that little crystals build up at numerous places and with perhaps various crystallographic orientations. As the mean film thickness increases, neighboring crystallites touch each other and presumably form a somewhat loosely packed spongy structure.<sup>8</sup> As the mean thickness continues to increase, the deeper-lying atoms or crystallites are subjected to stronger forces to rearrange into larger crystals and into shapes and orientations leaving a smaller net volume of intercrystalline space.<sup>12</sup> In general, the rate and extent of such an annealing or rearranging process are functions of time, of temperature (during and after production), of substrate structure, and of various conditions of the evaporation, e.g., sanitation of the substrate, rate of condensation, pressure, and type of residual gas present.<sup>13</sup> Because of the intercrystalline space, the average density near the surface is less than the normal bulk value and presumably increases with depth (excepting the uncertain region at the substrate interface). The phrase "loose packing" shall be used to refer to this type of attenuated average density.

<sup>12</sup> We assume that the x-ray scattering from the aggregate of loosely packed (and/or partially oxidized) crystallites is essentially coherent as for a medium of gradually changing density but that is otherwise homogeneous.

<sup>13</sup> Perhaps some of the rearrangement results from the escape or ejection of gas or other impurity atoms that were entrained during the condensation.

That greater porosity exists for thin than for thick films is shown by M. S. Blois, Jr., and L. M. Rieser, Jr., *J. Appl. Phys.* **25**, 338 (1954).

Loose packing is also a characteristic of many ground and polished surfaces. In the grinding and polishing process, mechanical rupture and distortion occur for many hundreds of angstroms in depth, and on the surface there may be short-range physical transport of atoms, atom groups, or crystallites. The degree of attenuation of density depends generally upon the crystallite size (and shape). Perhaps very close to the surface, a layer of extremely small atom groups or crystallites is present in an essentially liquid or amorphous state having a higher average density (because of close packing) than obtains for the region of loose-packed larger crystallites immediately beneath.

#### Oxidation

Oxidation of a copper mirror also results in an attenuated density if the oxide forms a skin-layer on the general surface plane. A 70Å copper single crystal on a Formvar substrate has been observed<sup>14</sup> to oxidize ( $\text{Cu}_2\text{O}$ ) to a depth  $x$ Å in  $t$  minutes in oxygen at 20 mm Hg pressure at room temperature according to the relation

$$x = 4 + 6.5 \log_{10} t, \quad t > 2 \text{ minutes}, \quad (14)$$

which, after 4 hours, gives  $x=20$ Å, and a limiting growth thickness of about 50Å after many years.<sup>15</sup> A thick abraded copper specimen oxidized to a maximum depth of only 90Å below the general plane of the surface after 21 months exposure to pure dry oxygen at room temperature.<sup>16</sup>

Interior oxidation may also occur: Oxygen may penetrate through the intercrystalline space in the spongy aggregate structure and corrode the surfaces of the deeper-lying crystallites. Interior oxidation is no doubt largely responsible for the fact that the specific area<sup>17</sup> is appreciably greater than unity.<sup>18</sup> Such oxidation, if the oxide does not fluff (break loose), results in an increase in electron density but not as high density as the normal bulk value for pure copper.

The copper mirrors of the present study were removed from the evaporation chamber, taken to another room

<sup>14</sup> A. H. White and L. H. Germer, *Trans. Electrochem. Soc.* **81**, 305 (1942). See also W. E. Campbell and U. B. Thomas, *Trans. Electrochem. Soc.* **91**, 623 (1947).

<sup>15</sup> It is unlikely that any other type of corrosion is important. An extremely thin layer of  $\text{CuO}$  may form on the surface of  $\text{Cu}_2\text{O}$  without much consequence; some  $\text{Cu}_2\text{S}$  is probably also present but with a presumed small effect.

<sup>16</sup> W. E. Campbell and U. B. Thomas, *Trans. Electrochem. Soc.* **76**, 303 (1939).

<sup>17</sup> The specific area, studied in catalysis, is the ratio of the free surface to the area of the general plane.

<sup>18</sup> O. Beeck, *Revs. Modern Phys.* **17**, 61 (1945), and others, also suggest that the oxygen is adsorbed in the interior surface of evaporated metal films.

and mounted on the x-ray spectrometer. A minimum of about 15 minutes exposure to laboratory air was unavoidable before the curve was recorded. Some rearranging of atoms or crystallites in the surface and some oxidation, both during and after preparation, were inevitable.

### Specific Conjectures

With the above general conjectures as to the nature of our surfaces, we turn to specific models in an attempt to understand the difference between the experimental and three-media curves of Fig. 6.

First, we note that in the region  $\phi/\phi_c > 1$ , the experimental curve falls below the theoretical curve. (This discrepancy is also a characteristic of each of several moderately thick gold, silver and aluminum mirrors with glass substrates. Our studies with these surfaces are not yet complete.) One is first tempted to say that an appreciable part of the x-ray beam penetrates through the metal film to the metal-glass interface where the beam is refracted into the glass and is lost. Indeed, the ratio of refractive indices of copper and glass precludes total reflection from the copper-glass interface for  $\phi > \phi_{eglass}$ . However, appreciable intensity is theoretically reflected from the glass, as is evidenced by the interference pattern of the three-media curve of Fig. 6. The theoretical curve includes, of course, both refraction into and partial reflection from the glass but the net average effect yields a curve which is about the same as for pure infinitely thick copper.<sup>19</sup>

We note also a similar but smaller discrepancy with the glass mirror, Fig. 2, for which there is no substrate.

We conclude that the substrate is not responsible for the discrepancy (except the oscillations) between the experimental and theoretical curves of Fig. 6.

#### (A) General Reduction of Density

A general reduction of (electron) density throughout the entire copper, such as by uniform porosity or by uniform partial oxidation during the evaporation process, would result in a reduction of  $\delta$ .

If the 2000A film were pure copper with a uniform porosity such that the average density were about 8 instead of 8.936 g/cm<sup>3</sup>, this model would give the observed value of  $\delta$ . If instead, the entire 2000A film were completely oxidized and not loose packed, the expected  $\delta$  (for Cu<sub>2</sub>O) would be  $14.16 \times 10^{-6}$ , i.e., 20.6 percent less than for normal bulk copper. But if the oxidation of individual crystallites were not complete, so that the average electron density were about midway between the values for Cu<sub>2</sub>O and Cu, this partial-oxide model would account for the observed value of  $\delta$ .

<sup>19</sup> It is interesting to note that an incorrect three-media theoretical curve which takes into account only the real part of the amplitude factor  $a_n$ , Eq. (7), shows no oscillations and lies below the two-media curve in the range  $\phi > \phi_c$  by a few percent. The imaginary or phase factor raises the curve, and indeed, raises it a greater amount for thinner films in the range just beyond  $\phi_c$ .

But neither of these models, uniform porosity or uniform partial oxidation, would account for the discrepancies in the two regions  $0.6 \lesssim \phi/\phi_c < 1$  and  $\phi/\phi_c > 1$ . In fact, these regions would be emphasized as *separate* regions if the theoretical curve (Fig. 6) were drawn for  $\phi_i/\phi_c$  at a value a little less than 1.068—the new fractional difference curve would have a pronounced minimum in it near  $\phi/\phi_c = 1$  indicating the likelihood of *two* different types of surface peculiarities in addition to the uniform reduction of density.

It seems likely that uniform general reduction of density, while perhaps present to a certain degree, is not the dominating feature of the mirror surface.<sup>20</sup>

#### (B) Oxide Layer of Limited Depth and of Varying Density

A more promising model is the following. Assume, first, that oxidation is complete and uniform to a certain depth, with no loose packing in the oxide or in the underlying pure copper. Three-media theoretical curves for this model are shown in Fig. 7 for each of several oxide thicknesses.<sup>21</sup> The constants used in the calculations for these curves are listed in Table IV. The curve for 150A thickness gives  $\delta$  in good agreement with experiment, and also exhibits a reduced intensity, but not the right curve shape, in the  $\phi/\phi_c > 1$  region. The discrepancy in the  $\phi/\phi_c < 1$  region is reasonably well accounted for.

Examination of the curves of Fig. 7, keeping in mind the penetration of the x-ray beam as the angle of incidence increases, indicates that, if a very small amount of loose packing or fluffing of the oxide were allowed at the surface and if the sharp Cu<sub>2</sub>O—Cu interface were relaxed into a gradual transition region, a model could probably be found which would give good agreement with experiment. The theoretical curve for one trial six-media model is compared with the experimental curve in Fig. 7; the details of the model are indicated in the figure. Additional laminae are evidently needed to approximate the transition from Cu<sub>2</sub>O to Cu. Note that inclusion of the glass substrate introduces the oscillations, fainter now than in Fig. 6.

This model, with additional laminal media to approximate gradual changes in density, would be satisfactory if oxidation does, in fact, agree with this pattern. Let us review our *a priori* expectations: (1) the oxide on the surface of a single copper crystal is not expected to penetrate more than about 20A [from Eq. (14)] at room temperature; (2) an evaporated copper surface

<sup>20</sup> More or less uniform reduction of density was concluded by H. Kiessig, reference 7. See also references 11 and 13, and R. W. James, *The Optical Principles of the Diffraction of X-Rays* (G. Bell and Sons, Ltd., London, 1950), pp. 171–177.

<sup>21</sup> Each of the three-media curves of Fig. 7 contains interference maxima and minima in the region  $\phi/\phi_c > 1$  not included in the figure; e.g., the second maximum in the 150A curve appears just beyond  $\phi = 10^{-2}$  radian.

[If the imaginary (or phase) factor of Eq. (7) is deleted, the curves corresponding to those of Fig. 7 for 5 to 150A show a sharp minimum near,  $\phi_c(\text{Cu}_2\text{O}) = 5.32 \times 10^{-3}$  radian, and show very close agreement with the pure copper curve for  $\phi/\phi_c > 1.02$ .]



consists of single crystals perhaps 70Å or more in size; (3) the evaporated copper surface is probably somewhat spongy; and (4) interior oxidation is probably present. Although at somewhat elevated temperatures complete oxidation of evaporated copper takes place a hundred or so angstroms in depth,<sup>22</sup> there is some question whether *complete* oxidation takes place in many or any of the 70Å (or larger) single crystals at room temperature.

Experimental curves with fresh 2000A copper mirrors usually have essentially the same shape as curves recorded after several months exposure to atmospheric air at room temperature. Occasionally, however, after ageing a mirror, the curve shows some slight decrease in reflected intensity in the region  $0.3 \lesssim \phi/\phi_c \lesssim 0.95$ , but not in the region  $\phi/\phi_c \gtrsim 1$ . (This intensity decrease with age, or with temporarily elevated temperature, is much more pronounced with thinner films.) The change in the curve may indicate that further oxidation (or some fluffing) of the partially oxidized smaller crystallites near the extreme surface occurs, but, in terms of this model, oxidation does not appear to progress more deeply into the mirror surface after the first few minutes of exposure to atmospheric air.

With the depth and completeness of oxidation in some doubt, we proceed to an alternative model.

### (C) Reflection Trap

In the proposed spongy aggregate of copper crystallites, the average crystallite size increases, and the

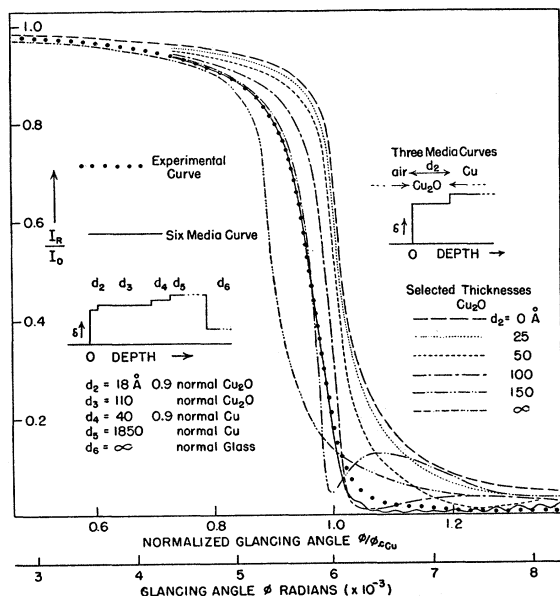


FIG. 7. Three-media reflection curves for homogeneous cuprous oxide on homogeneous copper, and one six-media curve for  $\lambda = 1.39\text{\AA}$ . The experimental curve is included for comparison.

<sup>22</sup> Garner, Gray, and Stone, Proc. Roy. Soc. (London) **A197**, 294 (1949), Disc. Faraday Soc. No. 8, 246 (1950); and M. Bound and D. A. Richards, Proc. Phys. Soc. (London) **51**, 256 (1939).

TABLE IV. Dispersion constants for  $\lambda = 1.39\text{\AA}$ .

Normal copper	Cu <sub>2</sub> O	Glass
$\rho = 8.936 \text{ g/cm}^3$	$6.0 \text{ g/cm}^3$	...
$\delta = 17.85 \times 10^{-6}$	$14.16 \times 10^{-6}$	$6.40 \times 10^{-6}$
$\phi_c = 20.54 \text{ min}$	18.29 min	12.3 min
$5.98 \times 10^{-3} \text{ rad}$	$5.32 \times 10^{-3} \text{ rad}$	$3.58 \times 10^{-3} \text{ rad}$
$\beta = 3.76 \times 10^{-7}$	$3.43 \times 10^{-7}$	$1.60 \times 10^{-7}$

intercrystalline space decreases, with depth into the surface. The lattice constant of Cu<sub>2</sub>O (4.26Å) is larger than that of copper (3.61Å), and the copper crystallite in the surface swells greatly as it changes to Cu<sub>2</sub>O. This is responsible for the possible fluffing of the oxide.<sup>23</sup> At some critical depth, the intercrystalline space first fills up with oxide. The mechanical forces involved in fluffing may at this depth effect a seal rather than continue fluffing which would now require a rather violent eruption of the large mass of material above the seal. If such a seal is formed, further free admittance of oxygen below the seal is stopped and oxidation here practically ceases.<sup>24</sup> The copper crystallites below the seal remain loose packed with a thin covering of oxide. With continued exposure to oxygen, the seal extends upward toward the surface, becoming thicker. Whether the seal reaches the surface before general fluffing above the seal occurs is not now important.

Formation of such a seal may be at least partially responsible for the rather sudden decrease after a minute or so in the observed rate of oxidation,<sup>14</sup> of oxygen take-up,<sup>25</sup> and/or of the heat of adsorption.<sup>26</sup> This subject is too complex for adequate treatment now.<sup>27</sup>

In terms of this model, the electron density may vary with depth somewhat as roughly sketched in Fig. 8 for pure but loose-packed copper and for partially oxidized copper. (In the figure, the heart of every partially oxidized crystallite is shown as remaining pure copper—this and other details of the figure are not to be taken too literally.) Although the term “seal” has been used and is indicated in Fig. 8, our interest is limited now

<sup>23</sup> F. C. Frank and J. H. van der Merwe, Proc. Roy. Soc. (London) **A200**, 125 (1950), suggest that, in general, if the molar volume of the oxide exceeds 115 percent of the molar volume of the metal, the oxide nucleates at several centers and may break away. K. Leu, Ph.D. thesis, University of London, 1951 (unpublished), reports that when exposed to laboratory air up to temperatures of 135°C, the cuprous oxide on single copper crystals grows as an amorphous layer. H. Frisby, Compt. rend. **226**, 572 (1948) and **228**, 1291 (1949), and others, find Cu<sub>2</sub>O on the (110) plane of a single copper crystal grows with orientation perfectly parallel to that of copper. It is yet difficult to know what happens.

<sup>24</sup> Oxidation below the seal continues but much more slowly, at a rate determined, perhaps, by the mobility of the cation (Cu<sup>+</sup>) through thick oxide. [See K. Hauffe, Prog. Metal Phys. **4**, 71 (1953).]

<sup>25</sup> J. A. Allen and J. W. Mitchell, Disc. Faraday Soc. No. 8, 309 (1950), and references.

<sup>26</sup> Beeck, Cole, and Wheeler, Disc. Faraday Soc. No. 8, 314 (1950), and references.

<sup>27</sup> See R. Gomer and C. S. Smith, *Structure and Properties of Solid Surfaces* (The University of Chicago Press, Chicago, 1953), for review of current status of this and related subjects.

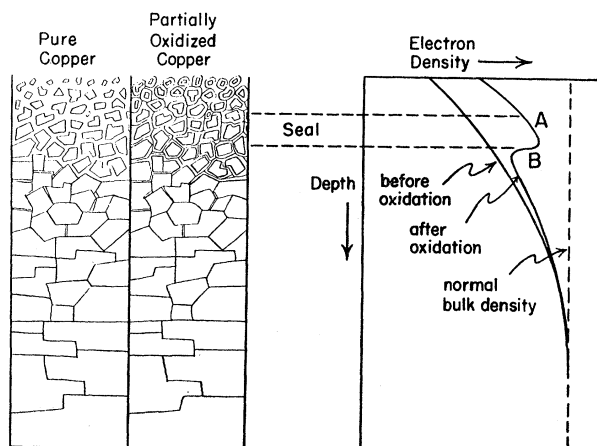


FIG. 8. Rough sketch of loose-packed surface structure of evaporated copper before and after partial oxidation. A seal of oxide is presumed to form; just below the seal the electron density is a minimum. The indicated loose packing and specific area are without doubt exaggerated for an evaporated copper surface produced and kept at room temperature.

to an electron density maximum and minimum whether or not an oxygen-impervious seal is present.<sup>28</sup>

The significant feature of this model is that part of the x-ray beam travelling upward in the mirror medium, suffers partial reflection at the underside of the density maximum (seal). For a certain range of angle, this beam, trying to break through the seal from underneath, is totally reflected back into the mirror where it is again reflected. The beam is thus partially caught in a "reflection trap."

The effect of such a reflection trap depends upon the details of the configuration of electron density in the surface. For five arbitrary configurations, each containing a density maximum and minimum, we have

<sup>28</sup> An electron density minimum may also be produced by the degree of close-packing of crystallites of gradually increasing size with depth. For example, on the extreme surface of optically polished glass, the "crystallite" size may be almost as small as individual molecules—a liquid-like surface with essentially no intercrystalline space. Also, in competition with oxidation or the liquid-like surface to effect the density maximum, we may have limited-depth intercrystalline adsorption of oils or other unidentified materials from the laboratory air. For copper, oxidation is possibly the principal effect; for glass, we cannot distinguish without better controlled conditions between the other two effects.

Professor T. J. Gray of Alfred University recently pointed out in a private conversation that the electrons which move from inside the copper (or oxide) surface to attach to the oxygen in chemisorption result in an excess of electrons at the surface (*n*-type material) and of holes inside the surface (*p*-type material). This contributes to the electron density maximum and minimum configuration but the relative magnitude of this contribution is probably small.

Another interesting possibility is the following. In the early stages of film deposition the copper crystallites may grow vertically and then "bridge over" enclosing holes at the substrate. If, as the film thickness increases, such vertical aggregation with subsequent lateral "bridging over" continues to occur, enclosing holes that are much smaller than those adjacent to the substrate, and if the more deeply embedded holes tend to collapse (except probably at the substrate), we may always have a reflection trap very close to the surface. This conjecture may be more reasonable than an interior oxide seal for evaporated metal surfaces.

evaluated Eq. (8); the resulting theoretical reflection curves are shown in Fig. 9. The constants used are listed in Table V; since  $\delta$  and  $\beta$  each varies linearly with electron density, they are listed together. The first configuration of Fig. 9 or Table V contains an exaggerated trap—an excessive reduction of effective electron density. The second, compared with the first, shows that the effect of the trap is sensitive to thickness  $d_2$ . The third and fourth configurations have shapes more like the experimental curve, with the minimum intensity in each case, however, too low and too narrow. The addition of two more laminae, the fifth configuration, helps in these regards. The  $\phi_c$  for the fifth configuration, is about  $5.83 \times 10^{-3}$  radian and the experimental value is  $5.67 \times 10^{-3}$ , a discrepancy in  $\delta$  of about 5 percent.

No doubt, with additional trial configurations, with generally smaller densities, and with perhaps more laminae to approximate gradually changing density, we could find a reflection trap configuration that would give excellent agreement with experiment in  $\delta$  and in curve shape. The significant conclusion now is that the agreeing configuration would probably be like the one we would guess for the proposed phenomenon—thus the reflection trap model is believed to be reasonable.

(Inclusion of the glass substrate as a seventh medium would introduce the interference oscillations but otherwise probably not seriously alter the curve shapes.)

The discussion has so far dealt with wavelength 1.39 Å. Curves recorded with  $\lambda = 1.54$  Å yield a  $\delta$  value ( $22 \times 10^{-6}$ ) which is 8.3 percent less than the theoretical value ( $24.05 \times 10^{-6}$ ) listed in Table II. The calculated penetration of these rays is somewhat, but not much, less than that of the 1.39 Å rays; but if the effect of the reflection trap is responsible for a large part of the discrepancy in  $\delta$ , a rather small change in penetration

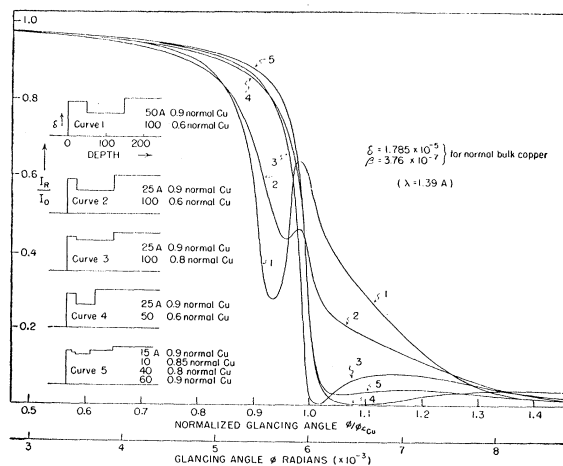


FIG. 9. The effect of a reflection trap in the surface. Curves for five different configurations of electron density are shown. The seal in the evaporated copper surface may be about 20 Å below the nominal surface plane to yield a curve in agreement with experiment.

may result in a rather large shift in the experimental  $\delta$ .<sup>29</sup> The observed shift is in the right direction to support the hypothesis of the reflection trap and its large influence in the percentage discrepancy in  $\delta$ .

### V. SUMMARY

The method of x-ray total reflection has been discussed for the study of certain surface properties of solids. Dispersion theory has been extended to treat any (small) number of stratified homogeneous media, and has been applied in an interpretation of experimental curves.

The measured refractive index term  $\delta$  is significantly less than the theoretical value (on the model of a single homogeneous mirror medium), and the experimental and theoretical curves are appreciably different in other regards. Three structural models of the surface have been discussed in an effort to account for the difference in the curves.

The discussion has been made in detail for a 2000Å thick evaporated copper film on a polished glass substrate. For this surface it is not reasonable that the copper film has only a general, uniform reduction of density; such a model accounts for only one discrepancy between the theoretical and experimental curves. A consistent accounting can be made, however, if the copper surface has oxidized completely to a depth of about 150Å with a small amount of loose packing or porosity on the surface and with a gradual transition region  $\text{Cu}_2\text{O}$  to  $\text{Cu}$ . The requisite complete-oxidation depth may be reduced somewhat if oxide is combined with some general porosity. But, since single crystals of copper are believed to oxidize at room temperature to a depth of only about 20Å, it seems likely that a third feature of the surface must be invoked. This feature is the so-called reflection trap, an actual minimum in the dispersion density about 20 to 50Å below the nominal surface plane.

Various conjectures have been proposed as to the physical cause of such a dispersion density minimum. Perhaps the oxide forms an interior oxygen-impermeable seal in a generally loose packed aggregate of copper crystallites. Or perhaps the film grows in thickness by vertical aggregation with subsequent lateral "bridging

<sup>29</sup> A tentative value of  $\delta$  from curves with gold films on glass,  $28.6 \times 10^{-6}$  for  $\lambda = 1.39\text{Å}$ , is 30 percent smaller than is predicted from Eq. (11) when the normal bulk density is assumed. In this case the penetration at  $\phi = \phi_c$  is, from Eq. (10),  $z_{1/e} = 60\text{Å}$ . If this reduction in  $\delta$  is caused by a reflection trap, the "seal" must be very close to the general surface plane.

TABLE V. Arbitrary electron density configurations: homogeneous laminae: reflection trap.  $\delta, \beta =$  fraction of the values for normal bulk copper, Table I.

Medium	First configuration		Second configuration		Third configuration		Fourth configuration		Fifth configuration	
	$d(\text{Å})$	$\delta, \beta$	$d(\text{Å})$	$\delta, \beta$	$d(\text{Å})$	$\delta, \beta$	$d(\text{Å})$	$\delta, \beta$	$d(\text{Å})$	$\delta, \beta$
1 (air)	...	0	...	0	...	0	...	0	...	0
2 (Cu)	50	0.9	25	0.9	25	0.9	25	0.9	15	0.9
3 (Cu)	0	...	0	...	0	...	0	...	10	0.85
4 (Cu)	100	0.6	100	0.6	100	0.8	50	0.6	40	0.8
5 (Cu)	0	...	0	...	0	...	0	...	60	0.9
6 (Cu)	$\infty$	1.0	$\infty$	1.0	$\infty$	1.0	$\infty$	1.0	$\infty$	1.0

over" enclosing holes which tend to collapse as they become more deeply embedded in the surface. The holes may be rather large only at a depth 15 to 50Å beneath the nominal surface plane (and perhaps at the copper-glass interface).

Curves for evaporated gold, silver, aluminum, and for optically polished glass were also mentioned with similar general conclusions. For the glass mirror (and perhaps to a certain extent for the metal mirrors) the maximum dispersion density in a loose packed surface may be caused by a dense amorphous surface layer or by a limited-depth adsorption of unidentified materials resulting from exposure to laboratory air.

The measurements to date have all been carried out under laboratory atmospheric conditions. These conditions do not allow satisfactory separation and control of the physical (and chemical) variables believed to be involved in the surface. For this reason, the method has been explored only qualitatively to date: We cannot yet choose a realistic combination of the three surface features for copper (a) uniform porosity, (b) an oxide layer of limited depth and of varying density, and (c) a reflection trap. However, under more controlled conditions of preparation and treatment of the surface, we can restrict the number and/or range of the variables at our disposal in selecting a surface model to be used in theoretical calculations. Then the method promises to be useful in surface studies of solids.

### VI. ACKNOWLEDGMENTS

The author is pleased to acknowledge his indebtedness to Mr. C. F. Dam, Mr. J. O. Porteus, and Mr. C. F. Hempstead for recording many of the curves, to Mr. Gerry Neugebauer, Mr. Robert Braden and the Cornell Computing Center for computations, and to Mr. Edmond Brown and Dr. E. L. Jossem for many pleasant and stimulating discussions.